Water Science & Technology

Water Science & Technology Vol 85 No 1, 515 doi: 10.2166/wst.2021.613

Optimization of multiple parameters for adsorption of arsenic (III) from aqueous solution using *Psidium guajava* leaf powder

Uma Sankar Behera [a,*], Prakash Chandra Mishra[b] and G. B. Radhika[c]

[a] Department of Chemical Engineering, GIET University, Gunupur, Odisha 765022, India
[b] Department of Environmental Science, FM University, Balasore, India
[c] Department of Chemical Engineering, B.V. Raju Institute of Technology, Hyderabad, India
*Corresponding author. E-mail: usb2007usb@gmail.com

USB, 0000-0002-1388-0401

ABSTRACT

The conventional method of water treatment using activated carbon from several sources has been focused on extensively in the last two decades. However, rare attention has been noticed on natural adsorbents such as plant leaves. Therefore, the *Psidium guajava* (guava) leaf has been investigated to understand its adsorption efficacy for Arsenic (III) [As(III)] in this study. The effect of process variables, e.g., pH, concentration of metal ion, adsorbent's particle size, and dosages, are evaluated. Experiments are carried out in batch mode, and the individual and combined parameter's impact on adsorption have been discussed. Fourier transform infrared spectroscopy (FTIR) and scanning electron microscopy (SEM) is used to characterize the adsorbent's surface. Freundlich and Langmuir's isotherms are used for adsorption equilibrium study. The adsorption parameters are optimized by establishing a regression correlation using central composite design (CCD) of response surface methodology (RSM). The analysis of variance (ANOVA) suggests a high regression coefficient ($R^2 = 0.9249$) for the removal of As(III). Particle size of 0.39 mm; adsorbent's height of 10 cm; metal ion concentration of 30 ppm, and pH 6 are optimized to remove 90.88% As(III) from aqueous solution. HCl is evaluated as a potential solvent for desorption of arsenic from the desorption study.

Key words: adsorption, ANOVA, concentration, desorption, optimization, *Psidium guajava*

HIGHLIGHTS

- Bio-adsorbent has significant potential to removal arsenic from wastewater.
- Metal uptake of the bio-adsorbent was high at initial period of batch process.
- Adsorption of arsenic is noticed to be highly pH-dependent.
- Desorption study reveals that HCl is a potential solvent for arsenic desorption.

GRAPHICAL ABSTRACT

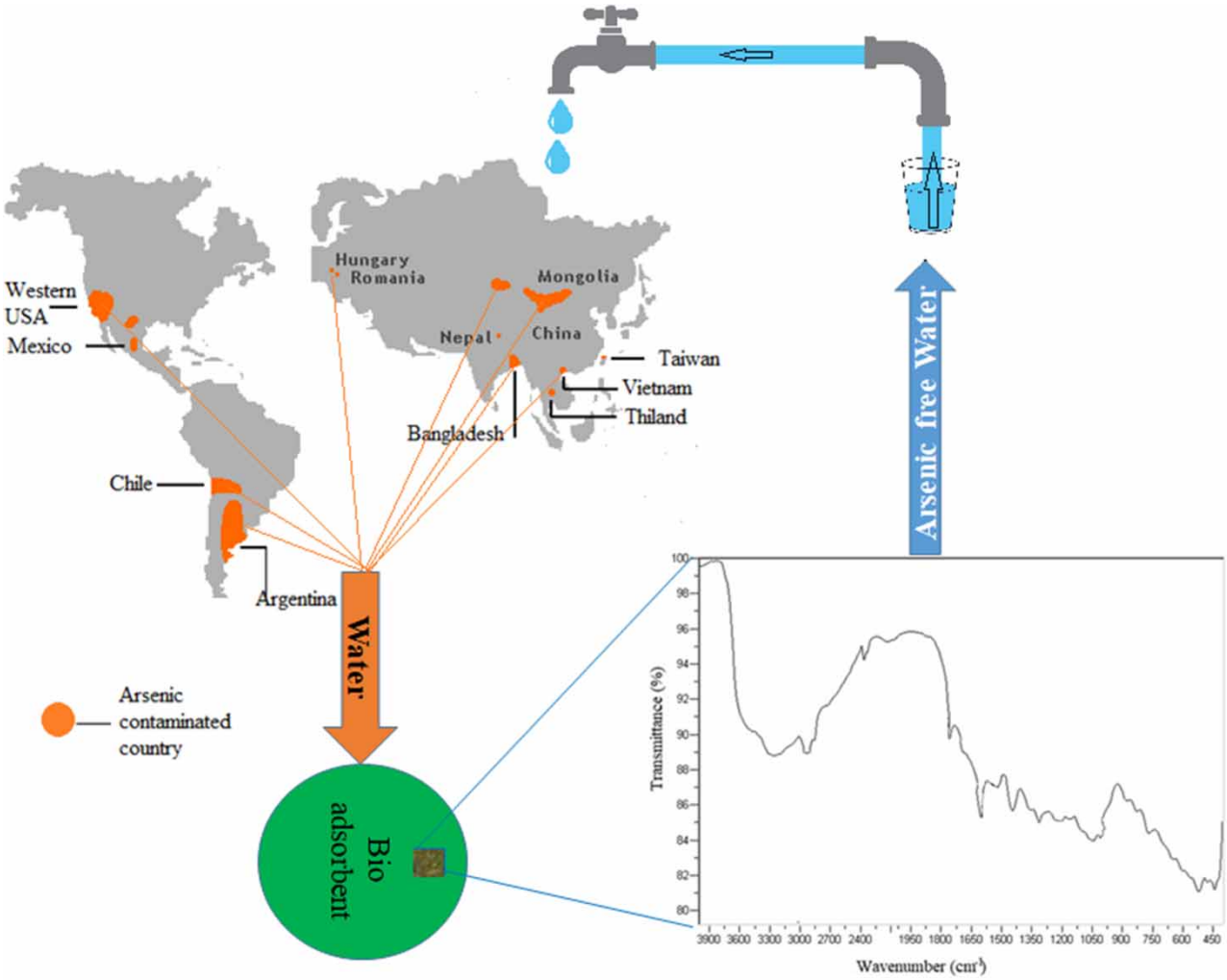

INTRODUCTION

Metalloid arsenic is found on the earth's crust in oxide form and enters the water body due to rock dissolution, which is highly poisonous. Researchers have found the increasing concentration of arsenic toxicity and its contamination in the groundwater in the recent era. Arsenic concentration in the groundwater is increasing rapidly due to: (a) excess utilization of the chemical fertilizer that containing arsenic, (b) utilization of pesticides containing arsenic, (c) waste disposal from paint and dye industries (i.e., for dye and paint production arsenic is used), (d) waste disposal from the glass industries (i.e., to make spiral glass, arsenic is used), (e) waste disposal of wood industries where arsenic is used to preserve the wood. In addition to the above, arsenic also can enter the water body through volcanic eruption and mining. The arsenic occurrence in water is endangering the life of aquatic flora and fauna and is very harmful if we consume it even in small quantities. Therefore, arsenic-contaminated water must be treated before being discharged to the water body. Arsenic occurrence in the consumable water is not at all desired. However, the presence of arsenic in drinking water is acceptable up to a limit of 10 μg/L as per the world health organization (WHO) and the Indian council of medical research (ICMR) (Kumar & Puri 2012). The presence of arsenic (III) [As(III)] beyond the permissible range may cause a health hazard, causing diseases such as black foot, nervous disorders, respiratory distress, kidney failure, cancer, and vascular diseases (Manju *et al.* 1998; Christen 2001; Zeng 2003; Goel *et al.* 2004; Chio *et al.* 2009). The research revealed that, commonly, arsenic occurs on the earth's surface in its trivalent and pentavalent states. However, trivalent arsenic [i.e., As(III)] is more harmful than pentavalent arsenic [i.e., As(V)] owing to its better

mobility higher toxicity properties. As(III) is relatively more strenuous to remove from arsenic-contaminated water than the As(V) (Genc *et al.* 2004). Despite many difficulties, a pretty good number of techniques have been developed by researchers for arsenic removal from arsenic-contaminated water, among which the chemical adsorption method has captured the attention of industries and is available commercially. It has been observed that researchers have used different adsorbents (inorganic, organic) to remove heavy metals from industrial wastewater, among which, mostly the inorganic adsorbent, has brought the attention of researchers towards it due to its availability. Many activated carbons from various materials have been developed and used to remove arsenic from wastewater containing arsenic (Gu *et al.* 2005). Chars obtained from wood and bark pyrolysis have been projected as suitable adsorbents for the removal of the heavy metals [e.g., As(III), Cd(II), and Pb(II)] from contaminated water, and achieved satisfactory result (Mohan *et al.* 2007). Peraniemi *et al.* (1994) have used modified zirconium-loaded activated carbon to remove arsenic from arsenic-contaminated groundwater as an adsorbent. They have reported that modified zirconium-loaded activated carbon could remove up to 75% of arsenic from arsenic-contaminated water. In addition to water purification, activated carbon is used to remove antimony and arsenic from copper electro refining solutions (Navarro & Alguacil 2002). Moreover, Navarro and Alguacil have reported that the ratio of solution to the activated carbon plays a vital role in removing arsenic from copper electro refining solution. Hence, it can be stated that carbon as an adsorbent (i.e., bio-adsorbent) has broad application industrially. Similarly, Genc *et al.* (2003) have used red mud (Bauxsol), a by-product of the aluminum industry, to remove arsenic from the arsenic-contaminated water. The red mud needs to be treated with seawater to achieve equilibrium pH before being used as an adsorbent. The treated red mud can then be used as an adsorbent to remove arsenic from arsenic-contaminated water. Their investigation revealed that arsenic adsorption from synthesized arsenic-contaminated water is significant when the pH of the solution is less, and the adsorbent dose is high. A higher amount of arsenic concentration in the water also affects the adsorption phenomena; comparatively, the presence of a low concentration of arsenic in the water results in better removal of arsenic from the water. Iron oxide has been reported as an efficient adsorbent in removing arsenic from wastewater containing arsenic (Katsoyiannis & Zouboulis 2004). However, the desorption of arsenic from iron oxide is not understood clearly. Iron-manganese binary oxide (FMBO) adsorbent has been used to remove As(III) and As(V) and achieved good arsenic removal efficiency, but the separation of the FMBO as metal ions by gravity sedimentation was quite tricky due to their small size (Wu *et al.* 2011). Mandal *et al.* (2013) have developed a novel hybrid material named zirconium polyacrylamide (ZrPACM-43). ZrPACM-43 was synthesized by mixing an aqueous zirconium oxychloride solution with a mixture of acrylamide. The above novel adsorbent was reported as reasonably fair in removing arsenic from arsenic-contaminated water. Raw laterite is also reported as an excellent adsorbent to remove heavy metals, including arsenic, from wastewater (Maiti *et al.* 2013).

Ngah & Hanafiah (2008) reported that plant waste could be used as an adsorbent to remove heavy metals, including arsenic, from wastewater. The neem leaves composite $MnFe_2O_4$ was used as an adsorbent to remove arsenic and reported that it could remove more than 75% arsenic from arsenic-contaminated water (Podder & Majumder 2015). The research revealed that the bio-adsorbent contains some natural polymer that might be responsible for removing heavy metals from the contaminated water. The above statement made the researchers pay more attention to the natural adsorbent to find an alternative bio-adsorbent to remove heavy metals (i.e., arsenic, cadmium, lead, chromium, mercury) from wastewater containing those metals. Acharya *et al.* (2018) reported that chemically modified agriculture waste could be used as a potential adsorbent to remove heavy metal ions from contaminated wastewater. Gaur *et al.* (2018) have reported that soya bean seed powder has greater efficiency in removing lead heavy metals than arsenic when used as an adsorbent. They also communicated that chemically treated bio-adsorbent works better than untreated bio-adsorbent in removing the heavy metals from the wastewater. Likewise, eggshell, java, plum seed, solid tea waste, and pomegranate peel have been experimented with to understand those adsorbents' potential for removing arsenic from wastewater containing As(III). Eggshell and java plum seed could eliminate 78% to 87% of As(III) at pH 7. However, the As(III) removal percentage of solid tea waste and pomegranate peel from wastewater were reported as 74% and 65%, respectively (Shakoor *et al.* 2019). Sattar *et al.* (2019) have reported that pea nutshell biochar (made from pyrolysis of pea nutshell) has the potential to remove more than 90% of As(III) from arsenic-contaminated water. It is reported that treated bio-adsorbents have more potential to eliminate As(III) than the untreated ones.

The literature study reveals that significant work has been studied on the inorganic substances to use them as the adsorbent for removal arsenic from wastewater. However, low priority has been given to natural bi-adsorbent. The raw natural adsorbent or the treated form is economical compared to the inorganic adsorbent. It has better efficacy to adsorb heavy metal than

inorganic substances as it contains carbon components. There are few water treatment techniques used in practice, such as reverse osmosis, filtration, ion exchange, coagulation and precipitation to remove organic or inorganic impurities from the wastewater. The above-said methods require suitable infrastructure; they are uneconomical, generate toxic sludge, and have less efficacy than bio-adsorbents. Guava leaves are abundantly available locally, have a greater tendency to remove heavy metal, do not generate sludge, are technically feasible, efficiently work under normal operating conditions, do not require big infrastructure and are highly economical. Activated charcoal is also a suitable adsorbent. However, they are costlier compared to bio-adsorbent and not available in every part of the country. The cost of 1 kg of activated charcoal is more than Rs. 500, whereas the cost of 1 kg of bio-adsorbent is Rs. 4 to Rs. 30 (Agarwal & Singh 2017). Therefore, guava leaf powder can be considered an alternative adsorbent for removing impurities (inorganic/organic) from the wastewater.

The natural solid guava leaf powder is considered an adsorbent in the present study to understand natural adsorbent's performance in removing As(III) from wastewater. The present study's objective is to realize the performance of natural adsorbents made from guava leaves in the adsorption of As(III) from synthesized arsenic water. The guava leaf is abundantly available in nature with sufficient carbon contents, which may help adsorb heavy metals (Kamsonlian *et al.* 2012). Hence, guava leaf powder is considered as the alternative adsorbent for arsenic removal from arsenic-contaminated water. The solid guava leaf powder's practical utility as the arsenic removal agent is studied in a batch process. To understand the single and combined effect of various system variables, i.e., pH of the aqueous phase/aqueous solution, the particle size of the adsorbents, initial concentration of As(III) in aqueous phase, and dosages of adsorbent (i.e., bed height of the adsorbent) on the removal of As(III) from the arsenic-contaminated aqueous solution has been considered. The central composite design (CCD) matrix of response surface methodology (RSM) has been applied in the present work to optimize the parameter for As(III) adsorption from prepared aqueous phase using organic adsorbent in a batch process.

Freundlich and Langmuir's isotherms have been used for adsorption equilibrium study. The adsorption potential of the guava leaf powder is evaluated based on experimental data and conditions.

MATERIALS AND METHODS

Chemicals

The chemicals used during this investigation are analytical reagent (AR) grade and having good purity. Details of the chemical used in this investigation can be found in supplementary material, Table S1.

Plant details

Psidium guajava (guava) is an evergreen shrub that belongs to the Myrtaceae family of the plant kingdom. The shrub has a slender trunk with smooth green to red-brown bark. The fruit is generally oval and green to yellow in color. It is a common tropical fruit observed in many tropical and sub-tropical regions. Guava leaf is also oval in shape with an average length of 7–15 cm and 3–5 cm wide. Guava leaf is used for the treatment of stomach pain, diabetes, and wound healing.

Adsorbent's preparation method

The guava leaves are abundant on the campus of GIET University, Gunupur, Odisha. The leaves were collected and cleaned with distilled water several times to remove foreign particles, if any. Thereafter, the leaves were sun-dried for approximately 15 to 20 days to remove the moisture content within them. They were then dried in the muffle furnance at 100 °C for 3 h. The dried leaves were then milled into a mixture of fine powder with the help of a hand hammer. The coarse powder was then further divided into distinct sizes using analytical sieves and then kept in a stoppered bottle until use. The natural form of the adsorbent contain fine grooves and hence, enhances the metal uptake (Alwared & Jaber 2020). Similarly, the higher carbon contents of natural adsorbents could be another reason to make them better adsorbents (Kamsonlian *et al.* 2012). The proximate and ultimate analysis reports of the guava leaf powder are detailed in Table 1.

The above analysis report revealed that the adsorbent contains a significant amount of fixed carbon compare to other natural adsorbents such as rice husk (~6%) and bagasse fly ash (~20%); hence, the guava leaf powder can be considered as a better adsorbent compare to rice husk and bagasse to remove heavy metals from contaminated water. However, the processed adsorbents are further activated by KOH to increase the porosity before use in the treatment process. Table 2, containing the scope of the experiment, and the system variables were considered to carry out experiments.

Table 1 | The proximate and ultimate analysis report of adsorbent (guava leaf powder)

Proximate analysis		Ultimate analysis	
Substance	**Weight %**	**Component**	**Weight %**
Moisture content	6.1	Carbon	54.8
Volatile substance	59.8	Nitrogen	41.2
Ash content	10.3	Hydrogen	4.0
Fixed carbon	33.8	Sulfur	Nil

Table 2 | System variables considered to carry out experiment

System variable	Mesh (ASTM)	Average particle size in (mm)
(a) Diameter of adsorbent		
D_{P1}	30 + 35	0.55
D_{P2}	35 + 40	0.46
D_{P3}	40 + 45	0.39
D_{P4}	45 + 50	0.32
D_{P5}	50 + 60	0.27
(b) Static bed height of adsorbent (Hs) in cm	6,8,10,12,14	
(c) Initial metal ion concentration (C_i) in ppm	10,20,30,40,50	
(d) pH of the solution	2,4,6,8,10	

Preparation of As(III) stock solution

As(III) solution was synthesized by dissolving 1.32 g of As_2O_3 in 1 L of deionized water collected from the IC-Evoqua water system (Giri *et al.* 2013). The conductivity of the deionized water was measured to be 0.0 55 μS/cm, and the resistivity was 18.2 MΩ cm. The pH of deionized was measured as 7.1 with pH meter (PC 2700, EUTECH Instruments, USA) at 25 °C. Throughout the experiment analytical-grade reagents were utilized in all cases. The fresh stock solution was prepared between 10 to 50 ppm for each run. The stock solutions were added with 0.1 N HCl or NaOH solutions to achieve the desired pH value and understand the effect of pH on metal ions' adsorption.

Analytical method

FTIR investigation is carried out by the spectrometer (Agilent Carry 660, Agilent Technology, USA). For FTIR analysis, the sample was prepared by diluting the adsorbent to 5% in KBr and cast in a disk for analysis. After the adsorption, samples of the aqueous solution were analyzed with an atomic absorption spectrometer (AAS) (NexION 300X, Perkin Elmer, USA). AAS works with the phenomenon that atoms absorb radiation from a particular wavelength of light to get excited. It has four important components: a light source, an atomizer section for atomizing the sample, a monochromator for picking the wavelength coming from the target element, and a detector which converts the light wave into an electrical signal. It usually determines the concentration of As(III) in ppm level in the solution, and the volume of sample needed for this is 1 mL for a single analysis. The concentration of As(III) in each sample after adsorption has been determined and recorded by AAS at different time intervals.

Batch method adsorption study

The stock solutions were prepared within the desired range (10 ppm, 20 ppm, 30 ppm, 40 ppm, 50 ppm) by diluting with deionized water. 100 mg of adsorbent was added in 50 mL of As(III) solution of desired concentration at pH 5 in a 100 mL conical flask. The solution was agitated with a mechanical shaker at 25 °C for 10 h. At last, the adsorbent was isolated from the suspension using the filtration process for analysis of As(III) on its surface. The concentration of As(III) in the solution was measured before and after the adsorption. The concentration of arsenic in the solution before adsorption is denoted

as C_0 and after adsorption as C_e. The dry weight of the adsorbent is denoted as (W), and the volume of the solution is (V). The amount of metal adsorb at equilibrium (q_e) was calculated as per Equation (1)

$$q_e(\text{mg/g}) = \{(C_0 - C_e)V\}/W \tag{1}$$

The removal percentage (R %) of As(III) = Difference in arsenic concentration in the solution before and after adsorption/ initial arsenic concentration in the solution

$$R(\%) = (C_0 - C_e)/C_0$$

Each experiment during the batch study was repeated three times to get the assured value.

Dynamic column method adsorption study

Experimental setup and procedure

Figure 1 shows the schematic of the experimental setup of the present study. The setup consists of a cylindrical column (5) containing guava leaves powder. The cylindrical column is made up of Perspex glass of 5 cm diameter and 20 cm in height. A 100 mesh screen (7) at the bottom is fixed, supporting the packing material, i.e., the adsorbents, and preventing them from coming out through the outlet. The bottom of the column is given a conical shape for a smooth collection of processed water. A pump (2) was connected at the bottom of the storage tank (1) to pump water to the cylindrical bed at a constant flow rate of 4 m^3/hm^2. The liquid's flow rate was controlled by the controlled valve (3) connected to the rotameter to maintain a constant flow rate (4). A u-tube manometer (6) is connected to the two ends of the bed. An iron stand (9) was connected to provide support to the cylindrical bed. To collect the discharge water passes through the bed, a conical flask (8) was arranged at the bottom of the fixed-bed column.

A known amount of the solid guava leaf powder was taken to ascertain a desired static bed height in the cylindrical column. The batch process was adopted to study the impact of various operating parameters on the adsorption % of As(III). Experiments for adsorption of As(III) on the prepared adsorbent has been performed with different weighted amounts of adsorbent sample. Two liters of the aqueous solution with 10, 20, 30, 40, and 50 ppm of initial arsenic concentration were considered to carry out the experiment for a constant time duration, i.e., 1 h. After each batch process, the old sample was replaced by a freshly prepared new sample to carry out the new experiment. The residual concentration of As(III) in the solution was

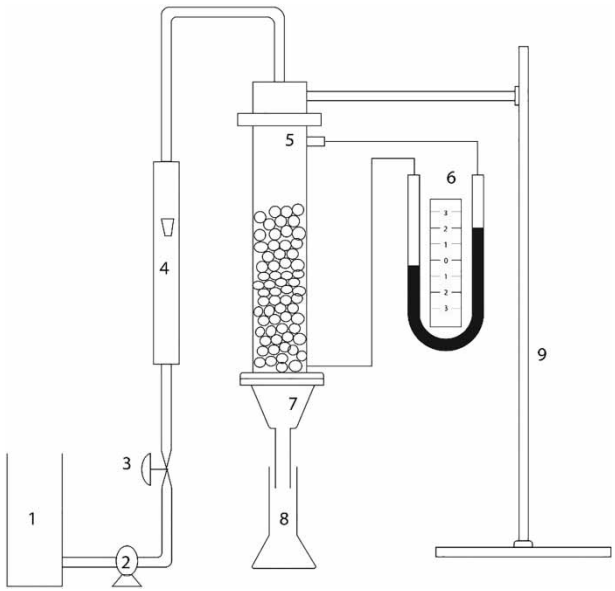

Figure 1 | Schematic of the experimental setup: 1, liquid tank; 2, water pump; 3, control valve; 4, rotameter; 5, column bed with adsorbent; 6, u-tube manometer; 7, mesh with conical base; 8, conical vessel; 9, iron stand.

analyzed using AAS. The solution (i.e., the arsenic-contaminated solution after passing through the adsorbent) was collected at the bottom of the cylindrical bed of the packed column. The collected solution was then allowed to pass through Whatman filter paper (Grade 1, Cat. No. 1001125, 125 mm Ø) to make it free from the adsorbent. As the batch process was followed, volume correction is neglected. The experiments have been performed at different concentrations, bed height of adsorbent, particle size, and pH of the solution.

RESULTS AND DISCUSSION

FTIR and SEM analysis of adsorbent

FTIR analysis of the adsorbent is carried out by the spectrometer (Agilent Carry 660, Agilent Technology, USA) with wave numbers ranging from 4,000 to 400 cm^{-1} to understand the surface chemistry (i.e., adsorbent's surface chemistry). FTIR analysis gives information about the functional groups present in the adsorbent. Figure 2(a) shows the FTIR analysis of the adsorbents before adsorption, and Figure 2(b) shows FTIR analysis of adsorbents after the adsorption. FTIR analysis reveals that the different functional group present in adsorbents is responsible for the accumulation of As(III) on the adsorbent's surface. FTIR analysis of adsorbents before adsorption shows that the bond at 2,925 cm^{-1} may assign to the C-H stretching of -CH_2- (Goel *et al.* 2005). Similarly, in the FTIR of adsorbents after absorption indicates that the peak located at 1,723 and 1,642 cm^{-1} corresponds to C=O stretching of carboxyl or amino group, which is very common in several biological compounds (Kamsonlian *et al.* 2012). The characteristic bond at around 1,582.09 cm^{-1}, 1,382.6 cm^{-1}, and 1,089.78 cm^{-1}, among which 1,382.6 cm^{-1} relatively stronger and indicates the presence of nitrate compounds. Similarly, vibration observed at 1,247 cm^{-1} represents stretching of the C-O bond of ester (Kamsonlian *et al.* 2012), commonly found in many natural compounds. It is observed that the shifting of the C=O group to the C-O group takes place at 2,731 cm^{-1}; this could be due to adsorption As(III) on adsorbent surfaces.

The images of the adsorbents are taken with scanning electron microscopy (SEM) (FEI Quanta 400 Field Emission Gun, Germany) to differentiate the adsorbent's surface before and after adsorption. Figure 3(a) and 3(b) shows the SEM images of adsorbents before and after adsorption. The magnification of the images before and after adsorption is slightly different, and this is considered to identify the surface changes more clearly. It has been observed that a small number of free masses are deposited on adsorbent surfaces after adsorption. The observed deposited free masses on the adsorbent's surface could be arsenic as no other elements except arsenic are present in the solution. The pore size of the adsorbent is also found to be reduced.

Adsorption studies of As(III)

Effect of pH and initial As(III) concentration

Figure 4 shows the adsorption percentage of As(III) from aqueous arsenic solution using guava leaves powder (i.e., adsorbent) with respect to initial ion concentration at different pH. The other parameter such as bed height (10 cm) and mean particle size (0.39 mm) were kept constant. Generally, As(III) appears in non-ionic (H_3AsO_3) and anionic ($H_2AsO_3^-$) forms in the pH range of 2.0–9.0 and 10–12, respectively (Ranjan *et al.* 2009). It was noticed that as the arsenic ion concentration in the aqueous phase increases, the adsorption percentage of arsenic ions decreases. This may be due to the unavailability of active sites on the adsorbent surface, but with the increasing pH of the aqueous solution, adsorption increases. Adsorption with variable pH is mostly influenced by metal ions concentration in the aqueous solution and the surface charge of the adsorbent. At the lower pH, the surface of the adsorbent is highly protonated; hence it can able adsorbed a comparatively lesser quantity of metal ions than high pH (Giri *et al.* 2013). Moreover, at low pH, OH radicals are the more oxidant for As(III). Therefore, there may be less removal of metal ions observed at low pH.

Effect of average particle size of adsorbent

Figure 5 shows the adsorption of As(III) from aqueous phase with respect to initial ion concentration for the different particle sizes. The bed height and pH were kept constant at 10 cm and pH 6, respectively. It has been noticed that with a decrease in particle size (0.55 mm–0.27 mm) of the adsorbent, the percentage of adsorption of metal ions increases. In other words, with a decrease in the size of the particle, adsorption increases. The increase in the adsorption percentage of metal ions with a decrease in the particle size is due to the increase in available surface area. The increase in the available surface area increases the active sites of the adsorbent; this could be the reason for enhancement for adsorption. However, maximum adsorption of As(III) in this investigation is noticed for particle size 0.39 mm, which may be due to its larger internal pore

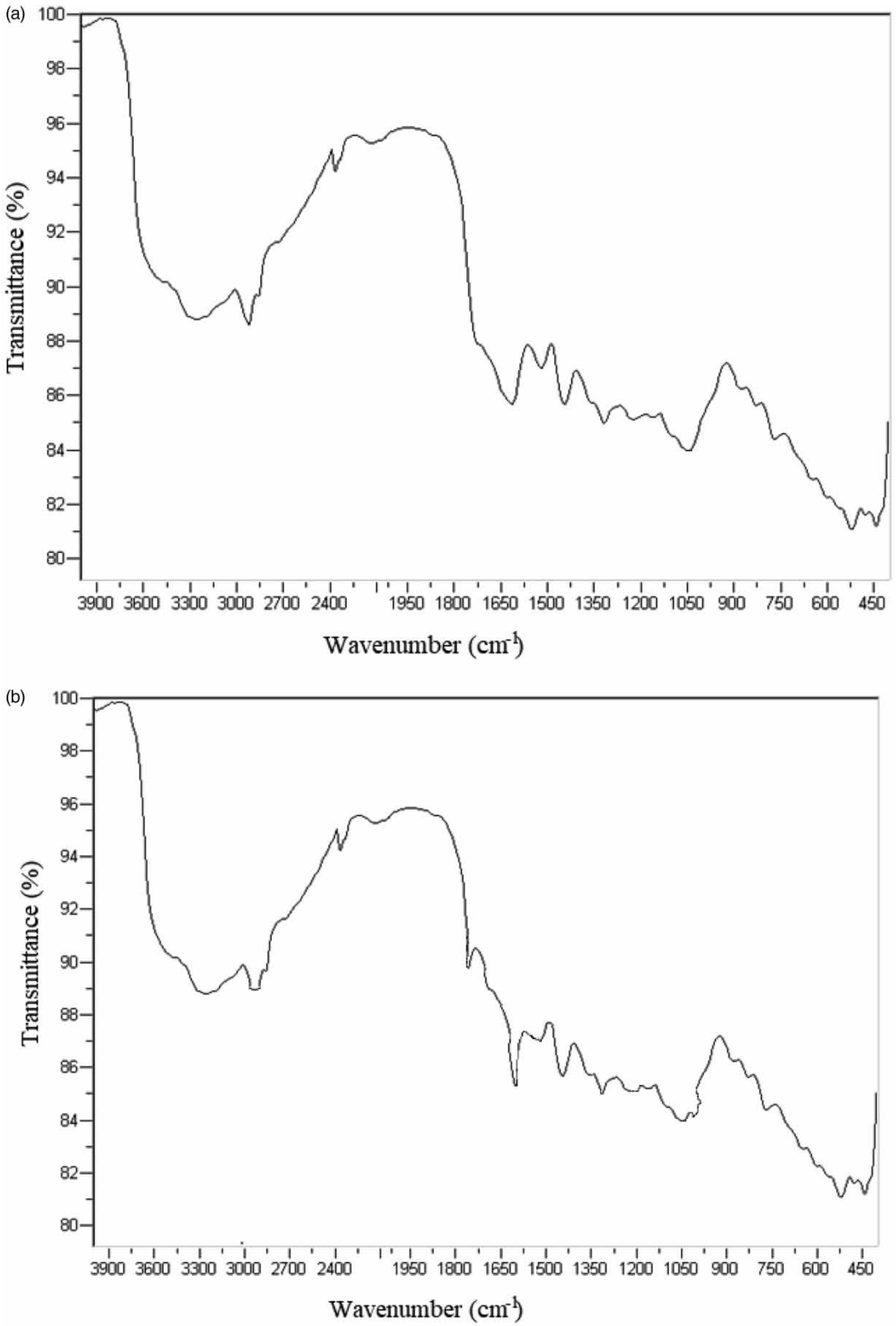

Figure 2 | FTIR analysis of adsorbent; (a) before adsorption, (b) after adsorption.

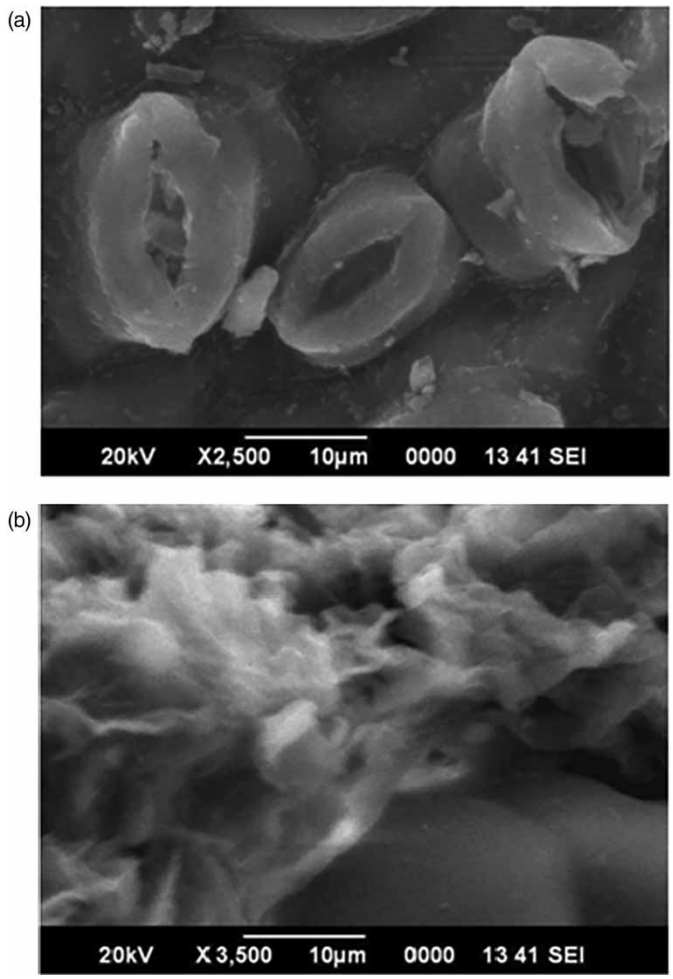

Figure 3 | SEM image of the adsorbent; (a) before adsorption, (b) after adsorption.

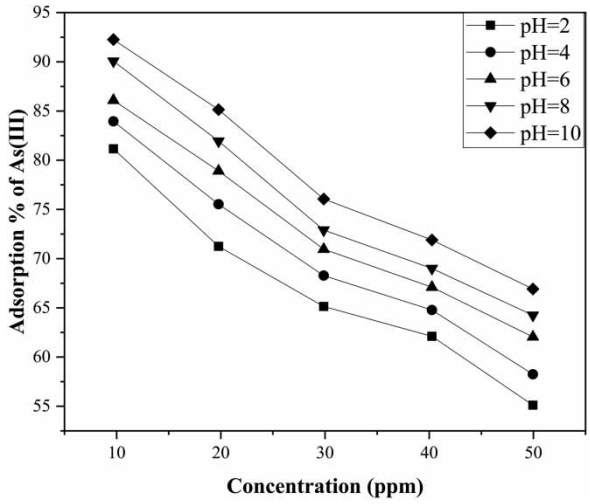

Figure 4 | Impact of pH on adsorption of As(III) at constant bed height (10 cm) and constant average particles size (0.39 mm).

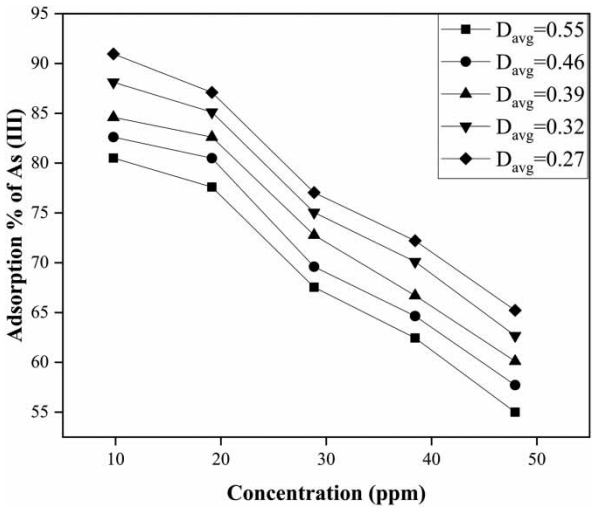

Figure 5 | Impact of particle size on adsorption of As(III) at constant bed height (10 cm) and constant pH of the solution (pH 6).

space. The inner pore surface area may bigger than the total outer surface area. Hence, the further reduction in particle size does not enhance adsorption percentage (Mondal *et al.* 2008); this may be why a 0.27 mm particle has a lower adsorption percentage than 0.39 mm. However, the reaction is time-dependent as diffusion of particle into pore takes time. Similarly, with the increase in the concentration of metal ions in the aqueous phase, the adsorption of metal ions decreases due to the decrease in active sites' availability on the adsorbent. This study is done to understand the effect of particle size on adsorption. However, a depth study can be done considering the BET surface area, total pore volume per gram of adsorbent, and adsorption time, which may be considered an objective of our subsequent investigation.

Effect of adsorbent dose (static bed height of adsorbent)

Figure 6 shows the adsorption % of As(III) with respect to initial ion concentration for variable static bed height of the adsorbent at a constant pH 6 and particle size of 0.39 mm. The adsorption percentage increases with an increase in the bed height for all the fixed bed height (Hs = 6 cm to Hs = 14 cm). Similarly, with the increase in the concentration of As(III) in aqueous solution (10 to 50 ppm), adsorption decreases. It has been noticed that with the increase in bed height of the adsorbent, adsorption percentage increases, which may be due to the increase in active sites of the outer surface area of the adsorbent group. However, at the lower concentration of the metal ions, adsorption increases due to the availability of more actives sites

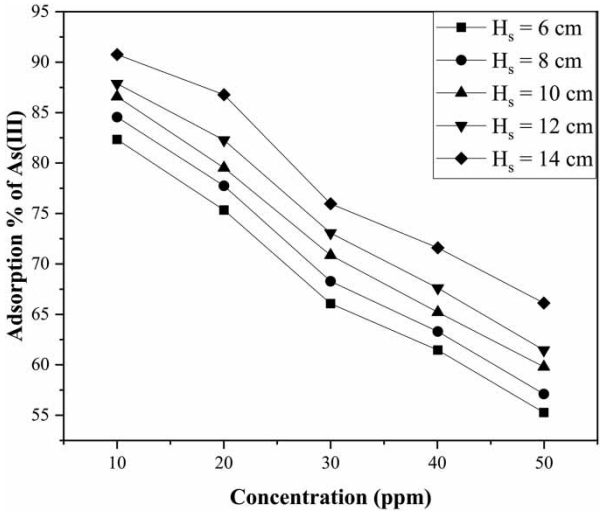

Figure 6 | Impact of static bed height on adsorption of As(III) at constant particle size (0.39 mm) and constant pH of the solution (pH 6).

on the adsorbent surface for limited metal ions. Likewise, with the rise in the concentration of As(III) in the aqueous phase, adsorption decreases due to the deposition of arsenic ions on the active sites (Goel *et al.* 2005). As the cost of the adsorption process depends on adsorbents, the static bed height must be optimized to minimize the cost. The optimized bed height for the recent investigation has been discussed in the subsequent section.

Development of regression model correlation

Central composite design (CCD) has been applied to construct a relationship between four variables (X_1, X_2, X_3, X_4) and As(III) adsorption percentage. The experimental scope and level of independent variables are listed in Table 3. A mathematical model (quadratic) is selected with the assistance of the software to find the adsorption percentage of As(III). Table 4 shows the design of the experiment and the actual result of the experiment.

The optimum value for the adsorption of As(III) is found to be 90.88%. The empirical mathematical model in terms of variables (X_1, X_2, X_3, X_4) for response Y [As(III) adsorption %] is given in Equation (2).

$$Y = 89.29 - 4.42X_1 - 6.54X_2 + 2.77X_3 + 0.68X_4 - 5.1X_1X_2 + 0.0073X_1X_3 - 1.08X_1X_4 + 8.25\,X_2X_3 + 0.93X_2X_4 - 0.54X_3X_4 - 16.7X_1^2 - 15.36X_2^2 - 8.75X_3^2 - 3.92X_4^2 \quad (2)$$

The plus symbol before the terms indicates a synergistic effect. Similarly, the minus symbol after the terms indicates the antagonistic effect. ANOVA (see Table 5) is used to fit the empirical model Equation (2) for statistical significance. R^2 is the degree of fitness of the model and required preferably higher value less than one but more than zero. The value of R^2, $R^2_{adjusted}$, and $R_{predicted}$ are found to be 0.9249, 0.9085, and 0.9148, respectively. The higher value of R^2 indicates a better fit for the model with the multiple variables. However, sometimes it does not happen, and $R^2_{adjusted}$ is calculated to compensate for increasing numbers of variables. As the R^2, $R^2_{adjusted}$, and $R_{predicted}$ are closed to each other, and it suggests good agreement with the experimental and predicted value.

Combined effect for adsorption of As(III)

Figure 7 shows the combined effect of bed height and particle size on As(III) adsorption at constant metal ion concentration 30 ppm and pH 6. The adsorption percentage of As(III) is optimum at particle size 0.39 mm and a bed height of 10 cm. With increasing the bed height, adsorption increases owing to the accessibility of more pores' space on the surface of the adsorbent. However, with a further increase in bed height, adsorption decreases. The decreased adsorption percentage with an increase in smaller particles could be due to the blocking of coarse particles' pores by the smaller particles (Dora *et al.* 2013). Similarly, adsorption decreases with increased particle size could be due to the relatively less active surface availability.

Figure 8 shows the combined effect of concentration and bed height on As(III) adsorption at constant pH 6 and particle size 0.39 mm. The adsorption percentage of As(III) is optimum, i.e., 90.88% at the metal ion concentration of 30 ppm and a bed height of 10 cm (see Figure 8). At lower concentrations of metal ions, adsorption decreases, which could be due to a decrease in diffusion rate. However, at higher concentrations of metal ions, diffusion increases, and hence, adsorption also increases. Adsorption increases with an increase in the concentration of metal ions but with further increase in concentration decreases, which may be due to a decrease in the active sites' availability on the adsorbent surface (Goel *et al.* 2005). With increasing bed height, adsorption increases, increase in adsorption could be due to accessibility of more active sites on the surface of the adsorbent (i.e., due to an increase in the adsorbent volume).

Table 3 | Level of independent variables

Variables	Symbol	$-\alpha$	-1	0	$+1$	$+\alpha$
Avg. particle size, D_{pav}, (mm)	X_1	0.27	0.32	0.39	0.46	0.55
Static bed height of adsorbent, H_s, (cm)	X_2	6	8	10	12	14
Initial ion concentration, C_i, (ppm)	X_3	10	20	30	40	50
pH	X_4	2	4	6	8	10

Table 4 | Design of experiments with the actual result of the experimental value

Run	X_1:D_{pav}, mm	X_2:H_s, cm	X_3:C_i, mg/L	X_4:pH	Y:% of adsorption
1	0.32	8	40	4	47.89
2	0.46	12	40	4	50.31
3	0.46	12	40	8	45.57
4	0.39	10	50	6	62.67
5	0.39	10	10	6	58.46
6	0.32	8	40	8	40.12
7	0.46	8	20	8	52.70
8	0.55	10	30	6	23.13
9	0.32	8	20	8	47.43
10	0.39	10	30	6	90.88
11	0.39	10	30	6	90.88
12	0.32	8	20	4	49.23
13	0.32	12	20	4	18.18
14	0.27	10	30	6	20.23
15	0.39	14	30	6	24.33
16	0.32	12	40	4	42.59
17	0.46	12	20	8	21.31
18	0.32	12	40	8	42.09
19	0.39	10	30	6	90.88
20	0.39	10	30	2	69.89
21	0.39	10	30	6	90.88
22	0.39	10	30	6	90.88
23	0.39	8	40	4	52.29
24	0.39	10	30	10	89.91
25	0.39	10	30	6	90.88
26	0.46	12	20	4	22.34
27	0.32	12	20	8	23.74
28	0.46	8	40	8	42.08
29	0.39	6	30	6	43.95
30	0.46	8	20	4	59.27

Figure 9 shows the combined effect of concentration of metal ions and pH on As(III) adsorption at a constant bed height of 10 cm and particle size of 0.39 mm. The optimum adsorption of As(III) is observed to be 90.88% at pH 6 and metal ion concentration 30 ppm. With the increase in the solution's pH, adsorption of arsenic increases initially, and with further increase in pH, adsorption decreases. The increase and then decrease in arsenic adsorption with the increase in pH could be owing to the rise of the solution's corrosive nature at higher pH, leading to damage to the adsorbent. Also, at low pH (i.e., at pH 6), the adsorbent's surface is highly protonated; this would be one reason for the adsorption of a relatively smaller quantity of metal ions at high pH than at low pH (Giri *et al.* 2013). The ANOVA for adsorption of As(III) from synthesized arsenic solution is given in Table 5.

The significance of the model can also be understood from the F (Fischer's) value and P (probability) value. Higher F value and lower *P*-value (<0.05) indicate a better fit for the experimental data model. The model F value is found to be 13.13, and most of the P was observed to be less than 0.05. Hence, the model is fitted with the experimental data. ANOVA analysis that was considered to explain the experimental data and response is reasonable.

Table 5 | ANOVA for adsorption of As(III)

Source	Sum of Squares	df	Means Square	F Value	*P*-value, Prob> F	Remarks
Model	16,616.20	14	1,186.87	13.13	<0.0001	Significant
X_1:Paticle size	426.73	1	426.73	4.80	0.0446	Significant
X_2:Height of bed	857.70	1	857.70	9.66	0.0072	Significant
X_3:Concentration	154.16	1	154.16	1.74	0.2075	
X_4:pH	9.25	1	9.25	0.10	0.7514	
X_1 X_2	3.87	1	3.87	0.044	0.8374	
X_1 X_3	8.178E-004	1	8.178E-004	9.208E-006	0.9976	
X_1 X_4	17.33	1	17.33	0.20	0.6650	
X_2 X_3	1,064.16	1	1,064.16	11.98	0.0035	Significant
X_2 X_4	13.68	1	13.68	0.15	0.7003	
X_3 X_4	4.62	1	4.62	0.052	0.8226	
X_1^2	8,950.40	1	8,950.40	100.77	<0.0001	Significant
X_2^2	6,460.11	1	6,460.11	72.73	<0.0001	Significant
X_3^2	2,097.83	1	2,097.83	23.62	0.0002	Significant
X_4^2	420.47	1	420.47	4.73	0.0460	Significant
Residual	1,332.34	15	88.82			
Lack of fit	1,332.34	10	133.23			
Pure error	0.000	5	0.000			
Cor total	17,948.54	29				
R^2					0.9249	
$R^2_{adjusted}$					0.9085	
$R_{predicted}$					0.9148	

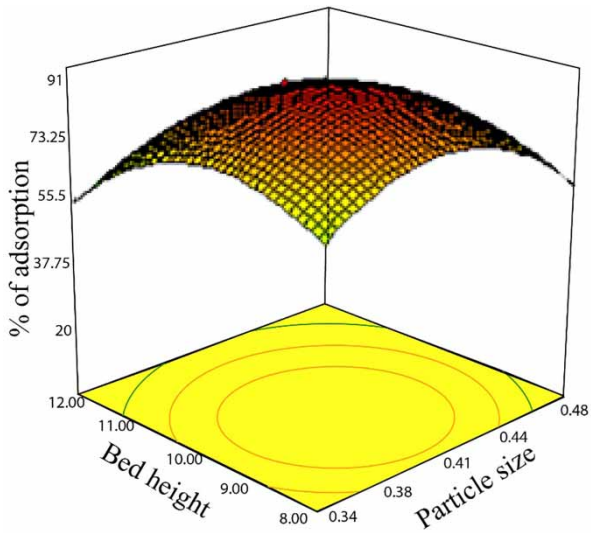

Figure 7 | Combined effect on adsorption of As(III) at pH 6 and metal ion concentration 30 ppm.

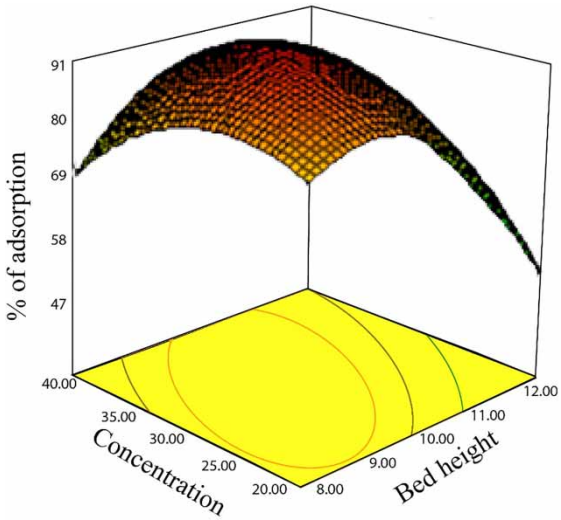

Figure 8 | Combined effect on adsorption of As(III) at pH 6 and particle size 0.39 mm.

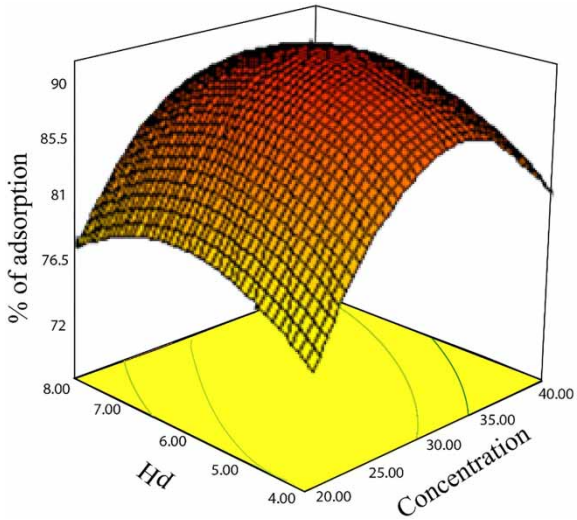

Figure 9 | Combined effect on adsorption of As(III) at particle size 0.39 mm and bed height 10 cm.

Optimization of adsorption of As(III)

The adsorption percentage of As(III) at different pH keeping constant particles size (0.39 mm) and bed height (10 cm) are measured. It has been observed that at pH 10, the adsorption percentage of As(III) is 89.91, whereas, at pH 6, it is 90.88% (see Table 4), which is higher than at pH 10. Figure 9 shows the combined effect of the parameter on the adsorption percentage of the As(III). It can be seen that maximum adsorption percentage is 90.88 at pH 6, and initial concentration 30 ppm (at fixed particle size: 0.39 mm; bed height: 10 cm). Figure 10 represents the predicted optimized region for the adsorption of As(III) at a fixed particle size and fixed bed height. The predicted value is in agreement with experimental value at same operational conditions. Hence, the most favorable adsorption conditions for the present adsorption process of As(III) by the guava leaf powder as an adsorbent have been ascertained at an average particle size of 0.39 mm; bed height of 10 cm; initial ion concentration of 30 ppm, and pH 6 to achieve the optimum adsorption of As(III) 90.88% for this design condition. Table 6 shows the optimized condition for As(III) adsorption.

Figure 11 shows that the plot predicted versus actual values, which lie mostly along the diagonal lines with little deviation. This indicates the quadratic model that has been used is fit for the process.

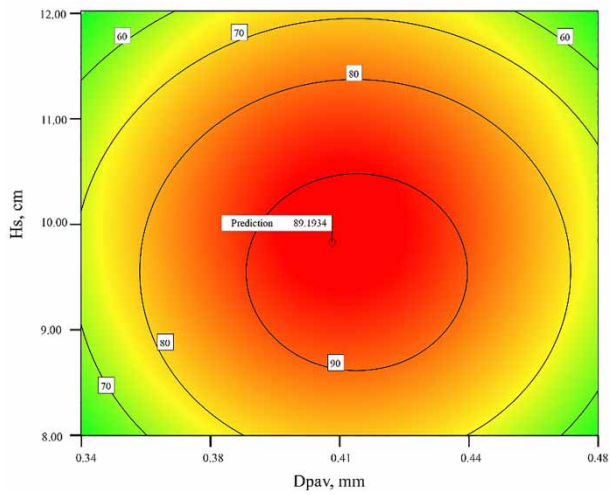

Figure 10 | Location of the optimum region for adsorption of As(III).

Table 6 | Optimized parameters for As(III) adsorption

				As(III) adsorption percentage (Y)	
D_{pav} in mm	H_s in cm	C_i, in ppm	pH	Predicted	Observed
0.39	10	30	6	89.1934	90.88

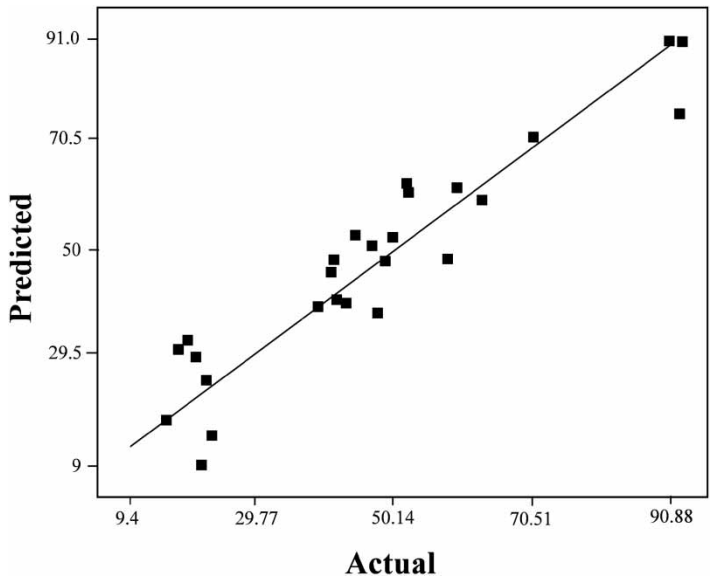

Figure 11 | Predicted *vs*. actual adsorption percentage of As(III).

Adsorption isotherm study

The researchers have used several existing models to describe the impact of concentration of arsenic on the porous surface of the adsorbents. The most commonly used models (Freundlich and Langmuir) are used to describe the experimental data. The arsenic adsorption isotherm followed the linearized Freundlich model, as shown in Figure 12. The relation between the metal

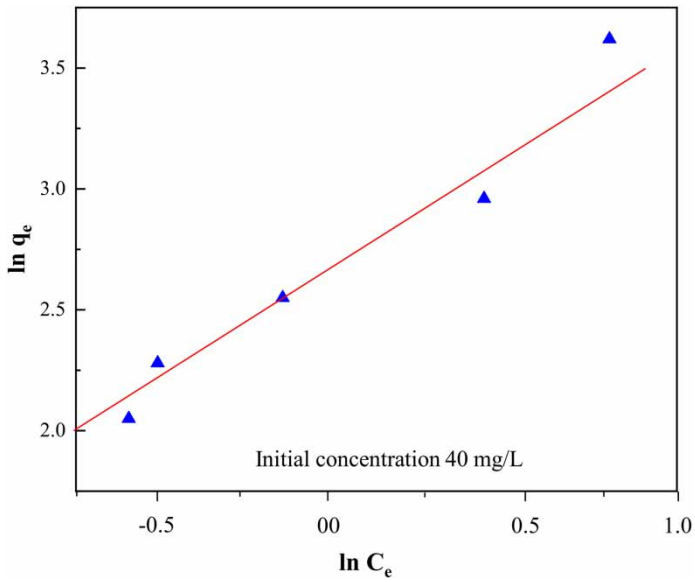

Figure 12 | Adsorption isotherm model of Freundlich for As(III) adsorption.

uptake capacity 'q_e' (mg/g) of adsorbent with the residual metal ion concentration 'C_e' (mg/L) at equilibrium is given in Equation (3)

$$\ln q_e = \ln K + 1/n \ln C_e \tag{3}$$

where the intercept ln$K$ is a measure of the adsorbent capacity, and the slope $1/n$ is the adsorption intensity. In the present investigation for Freundlich model, R^2 is found to be 0.9646. The values of the constants k and $1/n$ have been calculated as 13.367 and 0.934, respectively. The value of $1/n$ should be less than one for favorable adsorption, and the value is in line with the value found out for the present investigation, i.e., $0.934 < 1$.

According to the Langmuir isotherm, single layer adsorption of adsorbates takes place on the adsorbent surface. The uptake to the equilibrium liquid concentration (C_e) is given in Equation (4).

$$q_e = (K_L b C_e / 1 + b C_e) \tag{4}$$

The Langmuir adsorption isotherm is shown in Figure 13. The uptake of As(III) ions occurs on a homogeneous surface of guava leaf powder by single layer adsorption without the interaction between adsorbed molecules (Balasubramanian *et al.* 2009).

Table 7 shows that the Langmuir model is best suited for high linear regression coefficients R^2 (0.9818) of the experimental data for As(III) ions, which reveals that adsorption occurs at monolayers of solid–liquid phase interaction. The adsorption capacity (K_L) is found to be 118.22 mg of As(III) per gram of adsorbent (*Psidium guajava*). Table 8 shows the comparative study of arsenic adsorption on different investigators' different adsorbents with the present study.

Desorption study

The desorption phenomena of As(III) from used guava leaf powder is investigated using solvent elution (see Figure 14). The studies of desorption phenomena assist in understanding the adsorption mechanism and also to examine the firmness of the prepared adsorbents. During the solvent elution study, the adsorbent (i.e., guava leaf powder) was initially separated from the solution for further action (Mall *et al.* 2006; Suresh *et al.* 2011). The As(III) loaded on dry guava leaf powder of 0.2 g was then stirred at 150 rpm in a 250 mL beaker carrying 50 mL of test solution (0.1 N) each of hydrochloric acid (HCl), sulfuric acid (H_2SO_4), nitric acid (HNO_3), caustic soda (NaOH), and distilled water (H_2O) and of investigating concentrations at 25 °C for 10 h in a mechanical shaker. At the above-said conditions, the metal ions migrated from the adsorbents to the bulk solution of acid until the establishment of a new equilibrium exists. HCl is observed as a potential solvent for desorption of

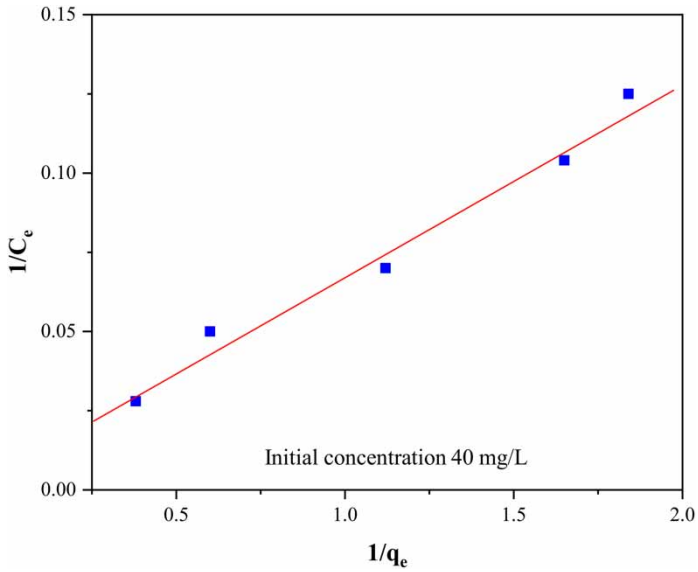

Figure 13 | Adsorption isotherm model of Langmuir for As(III) adsorption.

Table 7 | Adsorption isotherms parameter at pH 6 for As(III) removal

Freundlich model for As(III) at 25 °C			Langmuir model for As(III) at 25 °C		
R^2	K (mg/g)	1/n	K_L (mg/g)	b (L/g)	R^2
0.9646	13.367	0.934	118.22	0.015	0.9818

Table 8 | Comparative study for adsorption % of As(III) with the other adsorbents and activated guava leaf powder

Adsorbent	Adsorption % of As(III)	References
Kaolinite, surfactant modified	70	Li *et al.* (2007)
$Ti(SO_4)_2$	90	Sun *et al.* (2013)
Iron reduced graphite-oxide	9.10	Wang *et al.* (2014)
Moringaoleifera	71.3	Sumathi & Alagumuthu (2014)
Ferruginous manganese ore	72.58	Chakraborty *et al.* (2002)
Lamarck seed powder	60.21	Kumari *et al.* (2006)
Red mud	37.3	Altundogan *et al.* (2000)
Sea nodule polymetallic	90	Maity *et al.* (2005)
Activated red mud	37.5	Vithanage *et al.* (2007)
$Al_2O_3/Fe(OH)_3$	90	Suresh *et al.* (2011)
Java plum seed	78 to 87	Shakoor *et al.* (2019)
Solid tea waste	74	Shakoor *et al.* (2019)
Pomegranate peel	65	Shakoor *et al.* (2019)
Pea nutshell biochar	>90	Sattar *et al.* (2019)
Soya bean seed	42.74	Gaur *et al.* (2018)
Psidium guajava (guava leaves powder)	90.88	Present Study

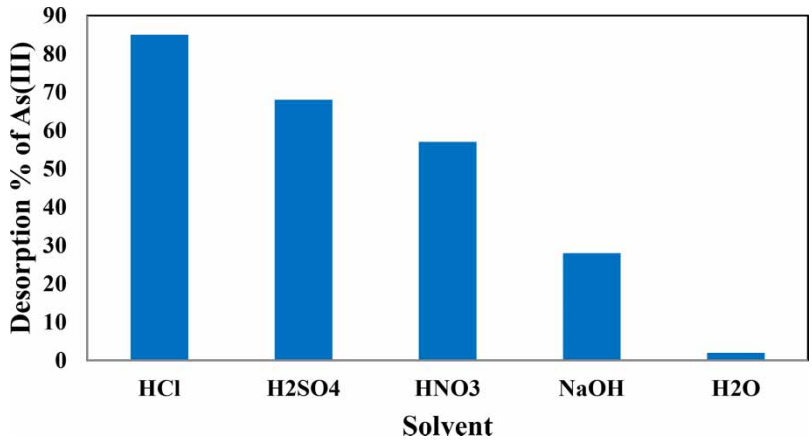

Figure 14 | Desorption of As(III) by different solvent at 25 °C.

As(III) compare to other solvents. The same kind of results were reported for the biosorption of, Ni(II), Cd(II), Co(II) and Zn(II) on the cellulose surface of the orange peels (Ajmal *et al.* 2000; Li *et al.* 2008). This specifies that ion exchange takes place during the adsorption process. Hence, the adsorbent's recovery of adsorbed arsenic ions is possible, and adsorbent can be reused, which is most important for industrial application.

CONCLUSION

In the present study, the guava leave powder has been taken as an alternative adsorbent to remove As(III) from the arsenic solution synthesized in the laboratory. RSM-based CCD and quadratic polynomial have been used to model and optimize the four process parameters on As(III) adsorption from arsenic-contaminated aqueous solution using guava leave powder. The four process parameters are listed as concentration of metal ion, the average particle size of the adsorbent, and the adsorbent's bed height and pH of the aqueous solution. The mathematical model equation is presented for adsorption of As(III) from an aqueous phase taking a group of data from the experiment and the ANOVA. The 3D response surface plots obtained from the models depict the impact of the process variables on As(III) adsorption. The model equation, which has given the predicted value, is in line with the observed values. Based on a quadratic polynomial, the average particle size of 0.39 mm; static bed height of 10 cm; initial ion concentration of 30 ppm; and pH 6 have been optimized as the most favorable levels of the variables to acquire the best adsorption (i.e., 90.88%) of As(III).

The results are encouraging for future application of guava leaf powder, and scale-up trials can be taken up for a possible commercial application. The data submitted may be useful for designing an economically feasible process using a batch reactor to remove As(III) from contaminated groundwater or industrial wastewater. The efficacy of the adsorbents in the removal of As(III) can be improved by being embedded with other suitable materials. The used adsorbent can be utilized for making plywood as it is a bio-adsorbent.

ACKNOWLEDGEMENTS

The authors would like to acknowledge the Sophisticated Analytical Instruments Facility and Department of Chemical Engineering, IIT Madras for providing SEM, FTIR and AAS analysis facilities. The authors also acknowledge the GIET University, Gunupur for providing laboratory facility to carry out the experiments. The authors also acknowledge Prem Sai (Tackle) for his help to draw the figure.

CONFLICT OF INTEREST

The authors declare that they have no known competing financial interests or personal relationships that could have appeared to influence the work reported in this paper.

DATA AVAILABILITY STATEMENT

All relevant data are included in the paper or its Supplementary Information.

REFERENCES

Acharya, J., Kumar, U. & Rafi, P. M. 2018 Removal of heavy metal ions from wastewater by chemically modified agricultural waste material as a potential adsorbent-A review. *Int. J. Curr. Eng. Technol.* **8**, 526–530.

Agarwal, M. & Singh, K. 2017 Heavy metal removal from wastewater using various adsorbents: a review. *J. Water Reuse Desalin.* **7**, 387–419.

Ajmal, M., Rao, R. A. K., Ahmad, R. & Ahmad, J. 2000 Adsorption studies on citrus reticulata (fruit peel of an orange): removal and recovery of Ni (II) from electroplating wastewater. *J. Hazard. Mater.* **79**, 117–131.

Altundogan, H. S., Tumen, F. & Bldik, M. 2000 Arsenic removal from aqueous solution by adsorption on red mud. *Waste Manage.* **20**, 761–767.

Alwared, A. I. & Jaber, W. S. 2020 Spiral path three phase fluidized bed reactor for treating wastewater contaminated with engine oil. *Appl. Water Sci.* **10**, 1–11.

Balasubramanian, N., Kojima, T. & Srinivasakannan, C. 2009 Arsenic removal through electrocoagulation: kinetic and statistical modeling. *Chem. Eng. J.* **155**, 76–82.

Chakraborty, S., Durej, V., Bhattacharjee, G., Maity, S. & Bhattacharjee, S. 2002 Removal of arsenic from groundwater using low-cost ferruginous manganese ore. *Water Res.* **36**, 625–632.

Chio, C. P., Lin, M. C. & Liao, C. M. 2009 Low-cost farmed shrimp shells could remove arsenic from solutions kinetically. *J. Hazard. Mater.* **17**, 859–886.

Christen, K. 2001 The arsenic threat worsens. *Environ. Sci. Technol.* **35**, 286–291.

Dora, T. K., Mohanty, Y. K., Roy, G. K. & Sarangi, B. 2013 Adsorption studies of As(III) from wastewater with a novel adsorbent in a three-phase fluidized bed by using the response surface method. *J. Environ. Chem. Eng.* **1**, 150–158.

Gaur, N., Kukreja, A., Yadav, M. & Tiwari, A. 2018 Adsorptive removal of lead and arsenic from aqueous solution using soya bean as a novel biosorbent: equilibrium isotherm and thermal stability studies. *Appl. Water Sci.* **8**, 1–12.

Genc, H., Tell, J. C., Mc Conchie, D. & Schuiling, O. 2003 Adsorption of arsenate from water using neutralized red mud. *J. Colloid Interface Sci.* **264**, 327–334.

Genc, H., Tell, J. C. & Mc Conchie, D. 2004 Increasing the arsenate adsorption capacity of neutralized red mud (Bauxsol). *J. Colloid Interface Sci.* **271**, 313–320.

Giri, A. K., Patel, R. K., Mahapatra, S. S. & Mishra, P. C. 2013 Biosorption of arsenic (III) from aqueous solution by living cells of Bacillus cereus. *Environ. Sci. Pollut. Res.* **20**, 1281–1291.

Goel, R., Kapoor, S. K., Mishra, K. Q. & Sharma, R. K. 2004 Removal of arsenic from water by using different adsorbents. *Indian J. Chem. Technol.* **11**, 518–525.

Goel, J., Kadirvelu, K., Rajagopal, C. & Garg, V. K. 2005 Removal of lead (II) by adsorption using treated granular activated carbon: batch and column studies. *J. Hazard. Mater.* **125**, 211–220.

Gu, Z., Fang, J. & Deng, B. 2005 Preparation and evaluation of GAC-based iron-containing adsorbents for arsenic removal. *Environ. Sci. Technol.* **39**, 3833–3843.

Kamsonlian, S., Suresh, S., Majumder, C. B. & Chand, S. 2012 Biosorption of arsenic from contaminated water onto solid Psidiumguajava leaf surface: equilibrium, kinetics, thermodynamics, and desorption study. *Bioremediation. J.* **16**, 97–112.

Katsoyiannis, I. A. & Zouboulis, A. I. 2004 Application of biological processes for the removal of arsenic from ground waters. *Water Res.* **38**, 17–26.

Kumar, M. & Puri, A. 2012 A review of permissible limits of drinking water. *Indian J. Occup. Environ. Med.* **16**, 40–44.

Kumari, P., Sharma, P., Srivastava, S. & Srivastava, M. M. 2006 Biosorption studies on shelled Morgana oleifera Lamarck seed powder: removal and recovery of arsenic from aqueous system. *Int. J. Miner. Process* **78**, 131–139.

Li, Z., Beachner, R., McManama, Z. & Hanlie, H. 2007 Sorption of arsenic by surfactant modified zeolite and kaolinite. *Mesopor Mater.* **105**, 291–297.

Li, X., Tang, Y., Cao, X., Lu, D., Luo, F. & Shao, W. 2008 Preparation and evaluation of orange peel cellulose adsorbents for effective removal of cadmium, zinc, cobalt and nickel. *Colloids Surf. A* **317**, 512–521.

Maiti, A., Thakur, B. K., Basu, J. K. & De, S. 2013 Comparison of treated laterite as an arsenic adsorbent from different locations and performance of best filter under field conditions. *J. Hazard. Mater.* **262**, 1176–1186.

Maity, S., Chakraborty, S., Bhattacharjee, S. & Roy, B. C. 2005 A study on arsenic adsorption on polymetallic sea nodule in the aqueous medium. *Water Res.* **39**, 2579–2590.

Mall, I. D., Srivastava, V. C., Kumar, G. V. A. & Mishra, I. M. 2006 Characterization and utilization of mesoporous fertilizer plant waste carbon for adsorptive removal of dyes from aqueous solution. *Colloids Surf. A* **278**, 175–187.

Mandal, S., Sahu, M. K. & Patel, R. K. 2013 Adsorption studies of arsenic (III) removal from water by zirconium polyacrylamide hybrid material (ZrPACM-43). *Water Resour. Ind.* **4**, 51–67.

Manju, G. N., Raji, C. & Anirudhan, T. S. 1998 Evaluation of coconut husk carbon for the removal of arsenic from water. *Water Res.* **32**, 3062–3070.

Mohan, D., Pittman Jr., C. U., Bricka, M., Smith, F., Yancey, B., Mohammad, J., Steele, P. H., Alexandre-Franco, M. F., Serrano, V. G. & Gong, H. 2007 Sorption of arsenic, cadmium, and lead by chars produced from fast pyrolysis of wood and bark during bio-oil production. *J. Colloid Interface Sci.* **310**, 57–73.

Mondal, P., Majumder, C. B. & Mohanty, B. 2008 Effects of adsorbent dose, its particle size and initial arsenic concentration on the removal of arsenic, iron and manganese from simulated groundwater by Fe^{3+} impregnated activated carbon. *J. Hazard. Mater.* **150**, 695–702.

Navarro, P. & Alguacil, F. J. 2002 Adsorption of antimony and arsenic from a copper electro refining solution onto activated carbon. *Hydrometallurgy* **66**, 101–105.

Ngah, W. W. & Hanafiah, M. M. 2008 Removal of heavy metal ions from wastewater by chemically modified plant wastes as adsorbents: a review. *Bioresour. Technol.* **99**, 3935–3948.

Peraniemi, S., Hannonen, S., Mustalahti, H. & Ahlgren, M. 1994 Zirconium-loaded activated charcoal as an adsorbent for arsenic, selenium and mercury. *Fresenius J. Anal. Chem.* **349**, 510–515.

Podder, M. S. & Majumder, C. B. 2015 Bacteria immobilization on neem leaves/mnfe2o4composite surface for removal of As(III) and As(V) from wastewater. *Arab. J. Chem.* **12**, 3263–3288.

Ranjan, D., Talat, M. & Hasan, S. H. 2009 Biosorption of arsenic from aqueous solution using agricultural residue 'rice polish'. *J. Hazard. Mater.* **166**, 1050–1059.

Sattar, M. S., Shakoor, M. B., Ali, S., Rizwan, M., Niazi, N. K. & Jilani, A. 2019 Comparative efficiency of peanut shell and peanut shell biochar for removal of arsenic from water. *Environ. Sci. Pollut. Res.* **26**, 18624–18635.

Shakoor, M. B., Niazi, N. K., Bibi, I., Shahid, M., Saqib, Z. A., Nawaz, M. F., Shaheen, S. M., Wang, H., Tsang, D. C., Bundschuh, J. & Ok, Y. S. 2019 Exploring the arsenic removal potential of various biosorbents from water. *Environ. Int.* **123**, 567–579.

Sumathi, T. & Alagumuthu, G. 2014 Adsorption studies for arsenic removal using activated moringaoleifera. *Int. J. Chem. Eng.* 1–6.

Sun, Y., Zhou, G., Xiong, X., Guan, X., Li, L. & Bao, H. 2013 Enhanced arsenite removal from water by $Ti(SO_4)_2$ coagulation. *Water Res.* **47**, 4340–4348.

Suresh, S., Srivastava, V. C. & Mishra, I. M. 2011 Isotherms, thermodynamics, desorption, and disposal study for the adsorption of catechol and resorcinol onto granular activated carbon. *J. Chem. Eng. Data* **56**, 811–818.

Vithanage, M., Senevirathna, W. & Chandrajith, R. 2007 Arsenic binding mechanism on natural red earth: a potential substrate for pollution control. *Sci. Total Environ.* **379**, 244–248.

Wang, C., Luo, H., Zhang, Z., Wu, Y., Zhang, J. & Chen, S. 2014 Removal of As(III) and As(V) from aqueous solutions using nanoscale zero-valent iron-reduced graphite oxide modified composites. *J. Hazard. Mater.* **268**, 224–231.

Wu, K., Wang, H., Liu, R., Zhao, X., Liu, H. & Qu, J. 2011 Arsenic removal from high-arsenic wastewater using in situ formed Fe–Mn binary oxide combined with coagulation by poly-aluminum chloride. *J. Hazard. Mater.* **185**, 990–995.

Zeng, L. 2003 A method for preparing silica-containing iron (III) oxide adsorbents for arsenic removal. *Water Res.* **37**, 4351–4358.

First received 28 July 2021; accepted in revised form 24 November 2021. Available online 8 December 2021